

Assessment of Tractable Cysteines for Covalent Targeting by Screening Covalent Fragments

László Petri, Péter Ábrányi-Balogh, Imre Tímea, Gyula Pálffy, András Perczel, Damijan Knez, Martina Hrast, Martina Gobec, Izidor Sosič, Kinga Nyíri, Beáta G. Vértessy, Niklas Jänsch, Charlotte Desczyk, Franz-Josef Meyer-Almes, Iza Ogris, Simona Golič Grdadolnik, Luca Giacinto Iacovino, Claudia Binda, Stanislav Gobec, György M. Keserű

Introduction

Targeted covalent inhibitors (TCIs) are important chemical biology tools and therapeutic agents.[1] TCIs form covalent bonds with nucleophilic residues, most often cysteine, but also others such as lysine, serine, threonine or tyrosine.[2] The advantages of TCIs include increased biochemical efficiency, prolonged duration of action leading to less frequent dosing, and an opportunity to target shallow binding sites, which were previously considered “undruggable”. [3] TCIs initially interact with the target by forming a noncovalent complex, followed by the reaction of the electrophilic functional group (a “warhead”) with the nucleophilic amino acid residue.[4] A closer look at electrophilic natural products reveals the presence of many reactive functionalities with diverse reaction mechanisms and varying intrinsic reactivities.[5] The most common TCI design strategy, however, pays less attention to the warheads[6] since they are typically attached to optimized noncovalent inhibitors.[7] By neglecting warhead reactivity optimization, this approach fails to enable the parallel optimization of covalent and noncovalent interactions that could contribute to the discovery of specific and safe covalent drugs.[8] Recent proteomic studies have suggested that the reactivity of cysteines is remarkably diverse in distinct proteins;[9] therefore, commonly used warheads should not be considered as the most suitable during the design process without experimental evaluation of their suitability. As mostly only computational approaches were used for the characterization of reactive cysteines,[6b,10] screening a diverse set of covalent fragments[11] represents an experimental alternative to these methods. Therefore, in contrast to previous studies,[12] our objective was not only to compare warheads reactivity, but to investigate the reactivity and accessibility of targeted cysteines with a set of covalent fragments, covering a suitable range of reactivity. To avoid the influence of noncovalent contributions, we equipped a single scaffold with a variety of warheads, composing a reactivity mapping toolbox. The constructed electrophilic fragment library was first characterized with experimental reactivity descriptors, aqueous stability and amino acid specificity information. These data confirmed their cysteine specificity and the range of reactivity covered. Then, we screened the library against proteins having different levels of functional and structural complexity (MurA, MAO-A, MAO-B, HDAC8, the immunoproteasome, and KRASG12C). Comparative profiling demonstrated that it is possible to pinpoint reactivity- and accessibility-based specificity caveats for the individual target. Furthermore, the study suggested the optimal warheads for the design of covalent inhibitors for a target of interest.

Results and Discussion

Mapping library design and characterization

To investigate the reactivity of different warheads in an unbiased way, we equipped the 3,5-bis(trifluoromethyl)phenyl group, a chemically stable and common motif in medicinal chemistry,[13] with different warheads. There are specific advantages of this scaffold. The limited size and complexity of the 3,5-bis(trifluoromethyl)phenyl fragment, which forms minimal noncovalent protein-ligand interactions, allowed screening against structurally diverse targets. Electron withdrawing properties and the orientation of the trifluoromethyl groups enhance the electrophilic character of the warheads. Therefore, functional groups with lower reactivity could also be investigated. After the proper analysis of the most common cysteine-targeting warheads,[6] we selected 28 covalent fragments representing 20 warhead chemotypes (Figure 1), with an average heavy atom count of 19 ± 2 and a molecular weight of 289 ± 36 g/mol. The library was assembled by acquiring compounds or their intermediates either from commercial sources or by synthesis (see the Experimental Section).

To test the reactivity range experimentally, we performed the thiol surrogate glutathione (GSH) reactivity assay (Table S1 in the Supporting Information),[12a,14] which showed that the library includes molecules from highly reactive fragments (2, 5, 6, 11, 12, 14, 15, and 24) to GSH nonreactive compounds (7, 8, 16, 17, 18, 22, and 28). Notably, the known reversible[15] binding of the cyano-acrylamide warhead (4) was confirmed. Next, the labelling efficiency and cysteine selectivity of the library members were evaluated against a nonapeptide model (KGDYHFPIC) containing multiple nucleophilic residues (Cys, His, Tyr, and Lys).[12a] Here, the cysteine selectivity of the fragments was confirmed. Furthermore, one should note that the fragments showed appropriate aqueous stability for biological testing (Table S1).

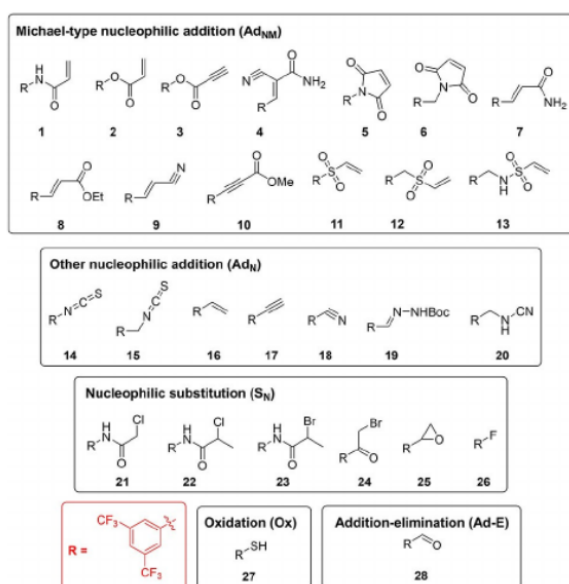


Figure 1. Covalent probes (1–28).

Profiling cysteines' reactivity and accessibility

Despite the usefulness of both surrogate model methods to obtain preliminary information on the reactivity and selectivity of warheads, we are well aware that these results do not always reflect events in complex biological systems. In our case, the results from the GSH reactivity assay and nonapeptide model were mostly, but not always, consistent with the results of enzyme assays (Tables 1 and S1).

Single concentration analyses against different protein targets were then performed to obtain preliminary reactivity profiles in a more complex system. As all library members had an identical scaffold, the reactivity heat map (Figure S1) suggested that the warhead chemotype had a significant impact on the labelling efficiency. Active warheads were identified in all chemical classes, and a trend that different tractable cysteines prefer different warhead chemotypes was also clear. A more detailed confirmation of the reactivity profiles was obtained by enzyme kinetic experiments.

Profiling on MurA

MurA (UDP-N-acetylglucosamine enolpyruvyl transferase) is a key enzyme in the biosynthesis of bacterial peptidoglycan precursors containing catalytic Cys115.[16] Single concentration screening showed that several fragments caused inhibition with residual activity (RA) between 0 and 50 % (Figure S1) and these were subjected to IC₅₀ measurements (Table 1). Notably, while in most cases the IC₅₀ values fell in the range of 38–399 μ M, we were able to identify compounds with low-micromolar inhibitory potencies (IC₅₀ values 0.5–14 μ M for compounds 5, 6, 11, and 27), indicating that a well-chosen covalent warhead might be able to cause a drastic increase in potency even with a non-optimized scaffold. The inhibitory potencies for all enzyme inhibitors in this manuscript are expressed as IC₅₀ values (Table 1), although the compounds are in most cases irreversible. The IC₅₀ values are therefore dependent on the assay conditions and particularly on the pre incubation period. Despite these limitations, the measured IC₅₀ values still allow relatively simple comparison of compounds within a series. However, additional methods were used in all cases to provide further information about the enzyme-inhibitor interactions. The covalent binding of the active compounds was confirmed by MS/MS studies, revealing that compounds 11 and 24 form covalent bonds with Cys115 located in the active site of MurA (Figure S2 and Table S2). Furthermore, STD NMR measurements were also performed to confirm the binding of fragments 6, 7 and 27 to MurA (Figure S3).

Table 1. IC₅₀ values of the electrophilic covalent fragments on MurA, MAO-A, MAO-B, HDAC8, and β5i subunit of the iCP.

	IC ₅₀ [μM] MurA	MAO-A	MAO-B	HDAC8	iCP β5i
1	164 ± 14	N.A.	N.A.	N.A.	N.A.
2	264 ± 23	N.A.	N.A.	24.42 ± 8.94	18.50 ± 9.19
3	N.A.	N.A.	N.A.	13.22 ± 3.90	N.A.
4	N.A.	61.2 ± 9.0	N.A.	> 50	N.A.
5	1.5 ± 0.2	0.34 ± 0.01	52.5 ± 10.7	0.51 ± 0.05	0.43 ± 0.53
6	11 ± 2.0	4.04 ± 0.24	N.A.	0.03 ± 0.01	N.A.
7	107 ± 11	16.4 ± 2.0	23.6 ± 1.2	4.00 ± 0.76	60.50 ± 3.53
8	N.A.	116.1 ± 22.8	58.9 ± 3.9	16.65 ± 6.78	N.A.
10	339 ± 31	N.A.	95.0 ± 9.0	34.96 ± 7.45	N.A.
11	13 ± 2.7	9.65 ± 1.53	N.A.	6.11 ± 1.78	5.90 ± 2.50
12	97 ± 10	13.53 ± 2.42	N.A.	1.95 ± 0.34	25.50 ± 17.68
15	381 ± 29	7.60 ± 1.84	N.A.	4.56 ± 0.40	12.50 ± 12.02
21	76 ± 8	314 ± 74	N.A.	> 50	N.A.
24	53 ± 7	N.D.	N.D.	1.02 ± 0.12	18.00 ± 8.0
27	14 ± 3	113 ± 29	N.A.	N.A.	5.00 ± 2.82

N.A. stands for „not active“, N.D. stands for „not determined“.

Profiling on monoamine oxidases

Monoamine oxidases A and B (MAO-A and MAO-B) are isoenzymes that catalyze oxidative deamination of monoamines. Known covalent inhibitors bind to the flavin adenine dinucleotide (FAD) cofactor. Notably, Cys321 and Cys323 in MAO-A and Cys172 in MAO-B, which are located in the active site or in close vicinity, could be targeted by electrophiles.[17] Activity profiling demonstrated that several fragments inhibited both enzymes, whereas some selectively targeted only one isoform (Table 1). We identified low micromolar MAO-A inhibitors (4, 6, 11, 12, 15, 21, and 27) with IC₅₀ values in the range of 4.0–314.0 · M, with no inhibition of MAO-B, and only one selective inhibitor of MAO-B (propiolate 10). Maleimide 5 was active on both isoforms, favoring MAO-A (IC₅₀=0.3 · M) over MAO-B (IC₅₀=52.5 · M). A detailed kinetic study revealed time-dependent and irreversible inhibition of fragments 6, 11, 12, and 15 (Figures S4 and S5). The covalent binding to MAO-A was confirmed by MS/MS proteomics, where vinyl sulfone 12 formed a covalent bond with Cys321 and Cys323 (Figure 2, more details in Figure S6 and Table S3). To the best of our knowledge, these are the first experimentally confirmed covalent fragments that bind to a specific cysteine and not to the FAD cofactor of MAO-A. Profiling on HDAC8 Histone deacetylase 8 (HDAC8) is an enzyme that plays a critical role in cell cycle progression by catalyzing the deacetylation of histones and a number of cytosolic proteins.[18] Considering the effects on cell reproduction, HDAC8 has attracted significant attention in oncology.[19] Numerous active fragments were identified in the HDAC8 inhibition screening (Figure S1). IC₅₀ values were determined for 11 active hits (Table 1). Notably, the acrylamide was clearly preferred in a more sterically hindered orientation, as 7 (IC₅₀=4.0 · M) outperformed 1, whereas the other acrylic fragment pair, esters 2 (IC₅₀=24.4 · M) and 8 (IC₅₀=16.7 · M), showed a similar potency. Maleimides were the only fragments active in the sub-micromolar range (IC₅₀ values of 0.5 and 0.03 · M for 5 and 6, respectively). The potencies of the other nine compounds were in the low-micromolar range (Table 1). In addition, the time dependency of inhibition was shown for the four most potent fragments (i.e., maleimides 5 and 6, vinyl sulfone 12, and haloacetophenone 24; Figure S7). The site of labelling was determined by MS/MS after tryptic digestion of the labelled protein samples with the most active compounds 5, 6, and 24. Maleimides 5 and 6 were anchored to cysteines 244 and 275, while haloacetophenone 24 labelled Cys275 only (Figure S8 and Table S4). Cys275 is in the proximity of the active site and its labelling might affect substrate binding, while fragments binding to Cys244 can be considered as allosteric modulators.[20] The broad activity profile obtained for this target

suggests that the reactivity of the available cysteines in HDAC8 allows the use of a wide range of warhead chemotypes.

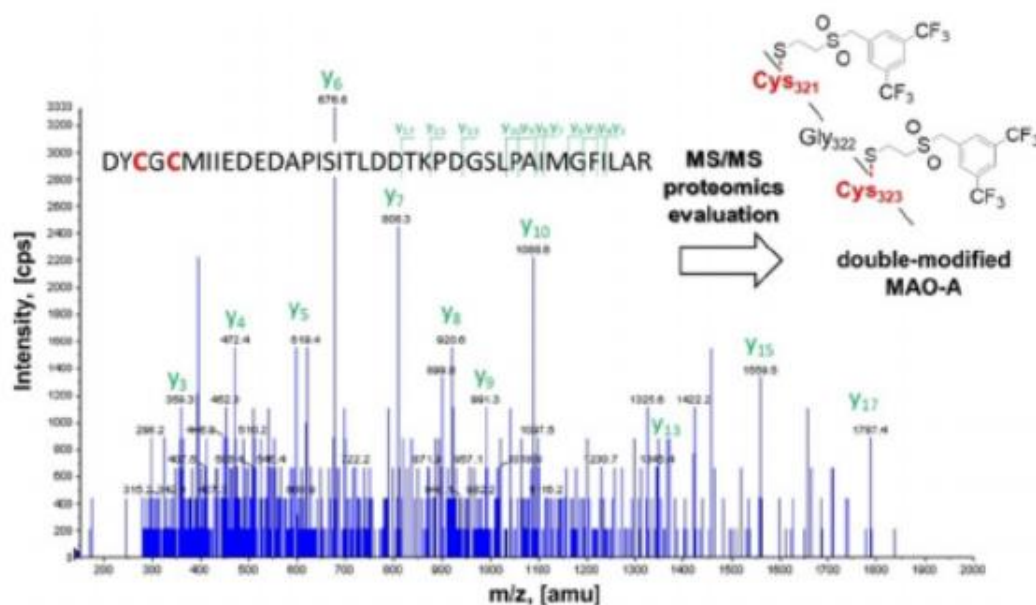


Figure 2. The MS/MS spectra of the enzyme-digested MAO-A peptide modified by covalent fragment 12 and the identified adduct

Profiling on immunoproteasome (iCP)

The immunoproteasome (iCP) is an isoform of the proteasome that is found mainly in cells of haematopoietic origin. Whereas the constitutive proteasome is a validated pharmacological target, individual subunits of the iCP are still being established as such.[21] Given that only a few inhibitors of the iCP are known, there is a need for novel chemical starting points. We found a lower number of hits in the case of the $\cdot 5i$ subunit of the iCP than in other cases (Figure S1). Eight fragments were characterized in terms of their IC_{50} values (Table 1), that is, the highly GSH-active chemotypes, including acrylester 2, maleimide 5, vinyl sulfones 11 and 12, benzyl isothiocyanate 15, and haloacetophenone 24. The most potent was maleimide ($IC_{50}=0.4 \cdot M$), while the IC_{50} values of the remaining compounds were found to be within a $5.0\text{--}25.5 \cdot M$ range. Similar to HDAC8, acrylamide 7 was identified as active ($IC_{50}=60.5 \cdot M$), whereas its structural pair acrylamide 1 did not show inhibition. In addition, intact MS measurements proved the covalent labelling with fragment 12 (Figure S9).

Profiling on KRASG12C oncogen mutant

KRAS is part of the RAS protein family of membrane-bound GTPases, which act as molecular switches. Somatic KRAS mutations are found in several cancers, with G12C (KRASG12C) being one of the most common mutations. Targeting Cys12 in the KRAS switch II pocket with covalent inhibitors represents a method of achieving selectivity over the wild-type protein to minimize toxicity.[22] The labelling efficiency of library members was investigated by Ellman's assay[23] as a direct estimation of the remaining free Cys ratio after incubating with the fragments (Figure 3). As KRASG12C has four cysteine residues, theoretically 25% labelling ratio could be measured by complete and selective binding to the targeted Cys12. Therefore, we

decided to set the labelling ratio (LR%) limit for 25%, which resulted in 13 hits, including acrylic compounds 1, 2, 4 and 7, maleimides 5 and 6, propiolate 10, vinyl sulfones 11 and 12,

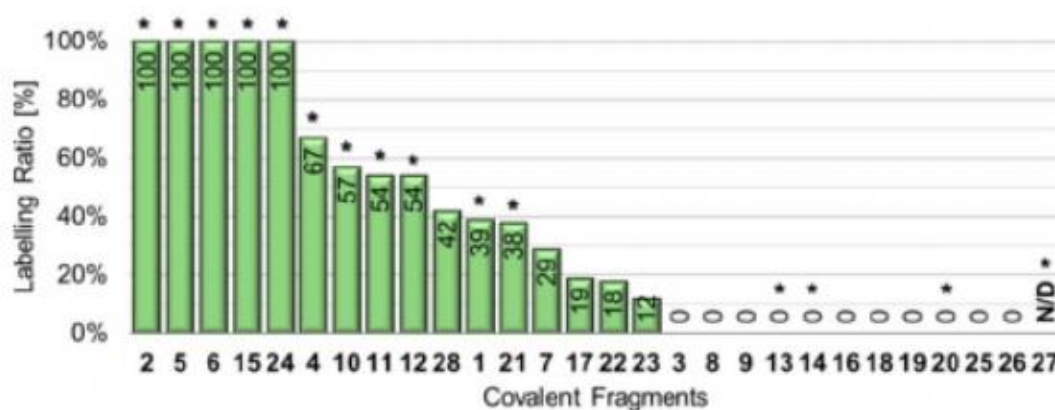


Figure 3. Results of Ellmann's assay and NMR measurements of KRASG12C. The Ellmann's assay results are presented as labelling ratio, the percentage efficacy ratio of the labelling. The covalent modifications confirmed by NMR measurements are indicated with a star on the top of the corresponding bar. N/D: not determined due to assay interference.

isothiocyanate 15, haloacetamide 21, haloacetophenone 24, and aldehyde 28. Because the Ellman's assay did not provide specific information on the labelling site, the compounds were subjected to ^{19}F -NMR and ^{15}N -HSQC NMR measurements to confirm covalent binding and identify the labelled residue (Figures S9 and S10). This methodology provided quick proof of the binding by comparing the ^{19}F shifts of the fragment in buffer as a reference with the fragment incubated with the protein. By comparing the results of both NMR methods, we found an almost perfect agreement between the more sophisticated ^{15}N -HSQC measurements and the ^{19}F -NMR protocol. There were only four outliers, that is, vinyl sulfonamide 13, isothiocyanate 14, and cyanamide 20, which were determined to be inactive in the Ellman's assay, but were proven to covalently label KRASG12C. Acrylamide 7 and aldehyde 28 were inactive in the NMR screen; however, these compounds showed labelling in the Ellman's assay. In every case where ^{19}F -NMR experiments showed binding, we were able to confirm the labelling by the ^{15}N -HSQC experiment. This observation suggests ^{19}F -NMR as an alternative to MS in cysteine mapping experiments with our library. In the case of KRASG12C, covalent labelling took place at Cys12 in all cases, with some compounds also labelling Cys118 as well.

Conclusion

To conclude, we report here the development of an electrophilic fragment library useful for the experimental evaluation of the accessibility and reactivity of cysteines, tractable for covalent inhibition. The wide range of thiol reactivity and high cysteine specificity of the fragments allowed us investigating a functionally and structurally diverse set of enzymes.

We confirmed that this methodology covers a wide range of targets. Furthermore, covalent binding was demonstrated with all enzymes that suggested particular warheads for developing specific TCIs. In the case of MAO-A, this analysis additionally revealed a new covalent

mechanism of inhibition by binding to the non-catalytic Cys321 and Cys323. Our results support the notion that there is no universal warhead available for different targets. In fact, the required specificity of TCIs necessitates not only optimized noncovalent interactions but also careful selection and tailoring of warheads. We suggest that warhead profiling by the approach presented here should constitute an important initial step in the identification of optimal warheads and development of TCIs.

Experimental Section

GSH reactivity and aqueous stability assay:[12a]

For glutathione assay 500 μ M solution of the fragment (PBS buffer pH 7.4, 10% acetonitrile, 250 μ L) with 200 μ M solution of indoprofen as internal standard was added to 10 mM glutathione solution (dissolved in PBS buffer, 250 μ L) in 1 : 1 ratio. The final concentration was 250 μ M fragment, 100 μ M indoprofen, 5 mM glutathione and 5 % acetonitrile (500 μ L). The final mixture was analysed by HPLC-MS after 0, 1, 2, 4, 8, 12, 24, 48, 72 h time intervals. In the case of fragments that were not detectable in a concentration of 250 μ M, the final concentrations were reversed, as 5 mM for the fragment and 250 μ M for GSH. Degradation kinetics was also investigated respectively using the previously described method, applying pure PBS buffer instead of the glutathione solution. In this experiment the final concentration of the mixture was 250 μ M fragment, 100 μ M indoprofen and 5 % acetonitrile. The AUC (area under the curve) values were determined via integration of HPLC spectra then corrected with internal standard. The fragments AUC values were applied for ordinary least squares (OLS) linear regression and for computing the important parameters (kinetic rate constant, half-lifetime) a programmed excel (Visual Basic for Applications) was used. The data are expressed as means of duplicate determinations, and the standard deviations were within 10% of the given values. The calculation of the kinetic rate constant for the degradation and corrected GSH-reactivity is the following. Reaction half-life for pseudo-first order reactions is $t_{1/2} = \ln 2/k$, where k is the reaction rate. In the case of competing reactions (reaction with GSH and degradation), the effective rate for the consumption of the starting compound is $k_{\text{eff}} = k_{\text{deg}} + k_{\text{GSH}}$. When measuring half-lives experimentally, the $t_{1/2}(\text{eff}) = \ln 2/k_{\text{eff}} = \ln 2/(k_{\text{deg}} + k_{\text{GSH}})$. In our case, the corrected k_{deg} and k_{eff} (regarding to blank and GSH containing samples, respectively) can be calculated by linear regression of the data points of the kinetic measurements. The corrected k_{GSH} is calculated from $k_{\text{eff}} - k_{\text{deg}}$, and finally half-life time is determined using the equation $t_{1/2}(\text{GSH}) = \ln 2/k_{\text{GSH}}$.

Oligopeptide selectivity assay:[12a]

For nonapeptide assay 2 mM solution of the fragment (PBS buffer pH 7.4 with 20% acetonitrile) was added to 200 μ M nonapeptide solution (PBS buffer pH 7.4) in 1:1 ratio. The final assay mixture contained 1 mM fragment, 100 μ M peptide and 10% acetonitrile. The samples were incubated at room temperature overnight. Based on the GSH reactivity the applied incubation time was 16 or 24 h. Fragments with less than 12 h half-life time against GSH were incubated for 16 h, the others for 24 h. Information-dependent acquisition (IDA) LC-MS/MS experiment was used to identify, whether the fragment binding was specific to thiol residues or not. Enhanced MS scan was applied as survey scan and enhanced product ion (EPI) was the

dependent scan. The collision energy in EPI experiments was set to 30 eV with collision energy spread (CES) of 10 V. The identification of the binding position of the fragments to the nonapeptide was performed by GPMAW 4.2. software. Relative quantitation of the nonapeptide-fragment covalent conjugates was calculated from the total ion chromatograms (based on peak area of the selected ion chromatograms).

MurA biochemical assay:[24]

MurA protein was recombinant, expressed in *E. coli*. The inhibition of MurA was monitored with the colorimetric malachite green method in which orthophosphate generated during reaction is measured. MurA enzyme (*E. coli*) was pre-incubated with the substrate UDP-N-acetylglucosamine (UNAG) and compound for 30 min at 37 °C. The reaction was started by the addition of the second substrate PEP, resulting in a mixture with final volume of 50 µL. The mixtures contained: 50 mM HEPES, pH 7.8, 0.005% Triton X-114, 200 µM UNAG, 100 µM PEP, purified MurA (diluted in 50 mM HEPES, pH 7.8) and 500 µM of each tested compound dissolved in DMSO. All compounds were soluble in the assay mixtures containing 5 % DMSO (v/v). After incubation for 15 min at 37 °C, the enzyme reaction was terminated by adding Biomol® reagent (100 µL) and the absorbance was measured at 650 nm after 5 min. Residual activities (RAs) were calculated with respect to similar assays without the tested compounds and with 5 % DMSO. The IC₅₀ values were determined by measuring the residual activities at seven different compound concentrations. The data are expressed as means of duplicate determinations, and the standard deviations were within 10% of the given values.

STD NMR of MurA:

The ¹H STD NMR spectra were recorded on Bruker Avance Neo 600 MHz (NMR Center, National Institute of Chemistry, Slovenia), using cryoprobe, at 25 °C. The pulse sequences provided in the Bruker library of pulse programmes were used. The samples were prepared in 90 % D₂O/10% [D₆]DMSO buffer containing 20 mM [D₁₁]Tris, 150 mM NaCl, and 0.049 mM [D₁₀] dithiothreitol; pD 7.4. Substrate UNAG was added at an enzyme/ substrate ratio of 1 : 5. All the spectra were recorded at an enzyme/ ligand ratio of 1: 100. The enzyme concentration was 0.004 mM, and the ligand concentration was 0.4 mM.

STD experiments were performed with a 6250 Hz spectral width, 16.384 data points, a saturation time of 2 s, a relaxation delay of 2 s, and 480 scans. Selective saturation was achieved by a train of 50 ms long Gauss-shaped pulses separated by a 1 ms delay. Water was suppressed by excitation sculpting. The on-resonance selective saturation of the enzyme was applied at 0.42 ppm. The off-resonance irradiation was applied at 30 ppm for the reference spectrum.

Protein labelling for MurA MS/MS proteomics:[12a]

For the MurA labelling experiment the 42 µM stock solution of MurA in 20 mM HEPES at pH 7.2–7.4 with 1 mM DTT was filtered through a G25 column and the medium was changed to 50 mM Tris with 0.005% Triton X-100 at pH 8.0. For the activation of the enzyme 1 mg UDPNAG was added as a solid to reach 40 mM concentration and the mixture was incubated at 37 °C for 30 min. Fragments were added from a 250 mM DMSO stock diluted in the labelling solution to 5

mM. The incubation was continued at 37 °C for additional 30 min. After the labelling, the mixture was purified on a G25 column.

MAO-A and MAO-B biochemical assay:

The effects of the test compounds on MAO-A and MAO-B were investigated using a fluorimetric assay, following a previously described literature method.[25] The inhibitory potency of the compounds was evaluated by their effects on the production of hydrogen peroxide (H₂O₂) from p-tyramine. The production of the H₂O₂ was detected using Amplex Red reagent in the presence of horseradish peroxidase, where a highly sensitive fluorescent product, resorufin, is produced at stoichiometric amounts. Recombinant human microsomal MAO-A and MAO-B enzymes expressed in baculovirus-infected insect cells (BTI-TN-5B1-4), horse-radish peroxidase (type II, lyophilised powder), and p-tyramine hydrochloride were obtained from Sigma Aldrich. 10-Acetyl-3,7-dihydroxyphenoxazine (Amplex Red reagent) was synthesised as described in the literature.[26]

Briefly, 100 µL 50 mM sodium phosphate buffer (pH 7.4, 0.05% [v/v] Triton X-114) containing the compounds and MAO-A/B were incubated for 30 min at 37 °C in a flat-bottomed black 96-well microplate. After the pre-incubation (30 min for the screening), the reaction was started by adding the final concentrations of 200 µM Amplex Red reagent, 2 U/mL horseradish peroxidase, and 1 mM p-tyramine (final volume, 200 µL). The production of resorufin was quantified on the basis of the fluorescence generated ($\lambda_{ex}=530$ nm, $\lambda_{em}=590$ nm) at 37°C over a period of 30 min, during which time the fluorescence increase linearly. For control experiments, DMSO was used instead of the appropriate dilutions of the compounds in DMSO. To determine the blank value (b), phosphate-buffered solution replaced the enzyme solution. The initial velocities were calculated from the trends obtained, with each measurement carried out in duplicate. The specific fluorescence emission to obtain the final result was calculated after subtraction of the blank activity (b). The inhibitory potencies are expressed as the residual activities (RA = $(v_i - b)/(v_0 - b)$), where v_i is the velocity in the presence of the test compounds, and v_0 the control velocity in the presence of DMSO. The IC₅₀ values were calculated using GraphPad Prism v8.0 software. The results are mean ± SEM of three independent experiments, each performed in duplicate. For determination of time-dependency, MAO-A was pre-incubated with the fragments for 5, 15 and 30 min and the assay was performed as described above. For the reversibility assay, MAO-A at 100-fold final concentration was incubated with the fragments at a concentration tenfold the IC₅₀ at 37°C (volume, 50 µL). After 30 min, the mixture was diluted 100-fold into the reaction buffer containing Amplex Red reagent, horseradish peroxidase, and p-tyramine hydrochloride. The final concentrations of all of the reagents and MAO-A were the same as in the assay described above. The reaction was monitored for 30 min. Control experiments were carried out in the same manner, where the inhibitor solution was replaced by DMSO. Clorgyline and harmaline were used as control irreversible and reversible MAO-A inhibitors, respectively. The results are mean ± SD of three independent experiments, each performed in quadruplicate.

Protein labelling for MAO-A MS/MS proteomics:

Human recombinant MAO-A (52 mM nominal concentration) in 50 mM sodium phosphate buffer at pH 7.8 together with 300 mM NaCl, 20 mM imidazole, 0.05% FOS-choline-12 and 40% glycerol was used for the labelling. The enzyme was expressed in *Pichia pastoris* and purified

following published protocols.[27]The MAO-A sample was quickly thawed from - 78°C to 37°C, and centrifuged (5 min at 7500 g) in order to remove the aggregated protein. MAO-A was buffer exchanged to 50 mM K₃PO₄ at pH 7.5 together with 0.25 % Triton X-100[28] and stored on ice. The electrophilic fragments were added in 0.5 µL DMSO (100 mM) to a 35–50 µL of the enzyme solution to reach 35- to 50-fold excess of the fragments. The samples were incubated at 4°C for 24 h.

HDAC8 biochemical assay:

Enzyme activity assay was executed in assay buffer (25 mM Tris·HCl pH 8.0, 50 mM NaCl and 0.001 % (v/v) P luronic F-68) in black half area 96-well microplates (Greiner Bio-One, Germany). For the initial screening 10 nM HDAC8 was pre-incubated with 250 µM of the indicated compounds for 2 h at 30°C. For IC₅₀ determination 10 nM HDAC8 was pre-incubated with a serial dilution of the indicated compounds for 1 h and with varying times for the time dependent IC₅₀ curves. The enzyme reaction was initiated by the addition of 20 · M Boc-Lys(TFA)-AMC (Bachem, Switzerland). After substrate conversion at 30°C for 1 h the reaction was stopped by adding 1.67 µM suberoylanilidetrifluoromethylketone (SATFMK). For time dependent IC₅₀ measurements the substrate conversion was stopped after 5 min. The deacetylated substrate was cleaved with 0.42 mg/mL trypsin to release fluorescent 7-amino-4-methylcoumarin (AMC), which was detected with a microplate reader (PHERAstar FS or BMG LABTECH) with fluorescence excitation at 360 nm and emission at 460 nm. IC₅₀ values were calculated by generating dose-response curves in GraphPad Prism 6 and fitting those to a four-parameter logistic model.

Protein labelling for HDAC8 MS/MS proteomics:

For covalent labelling 25 µM HDAC8 was treated with 250 µM of the indicated compound for 1 h at 30 °C in assay buffer as described above. After reaction the protein was precipitated by the addition of 10 % TCA and afterwards centrifuged at 18 000 g for 15 min. The supernatant was removed, and dry pellet was diluted in buffer (50 mM NH₄HCO₃, pH 7.8).

Immunoproteasome (β5i) biochemical assay:

The screening of compounds was performed at 100 µM final concentrations in assay buffer (0.01 % SDS, 50 mM Tris·HCl, 0.5 mM EDTA, pH 7.4). To each electrophilic fragment, 0.2 nM human iCP (Boston Biochem, Inc., Cambridge/MA, USA) was added and incubated for 30 min at 37 °C. Afterwards, the reaction was initiated by the addition of Suc-LLVY-AMC (a substrate to evaluate the activity of the β5i subunit of the immunoproteasome, Bachem, Bubendorf, Switzerland) at 25 µM final concentration. The reaction progress was recorded on the BioTek Synergy HT microplate reader by monitoring fluorescence at 460 nm (λ_{ex} = 360 nm) for 90 min at 37 °C. The initial linear ranges were used to calculate the velocity and to determine the residual activity. The results are means from at least three independent measurements. Standard errors for RAs were less than 15% in every case.

Compounds that showed average residual activity below 50 % in the RA determination assay were initially dissolved in DMSO, and then added to black 96-well plates in the assay buffer (0.01 % SDS, 50 mM Tris·HCl, 0.5 mM EDTA, pH 7.4) to obtain eight different final concentrations. The inhibitors were pre-incubated with 0.2 nM human iCP (Boston Biochem, Inc., Cambridge/MA, USA) at 37 °C 30 min, before the reaction was initiated by the Suc-LLVY-AMC substrate (Bachem,

Bubendorf, Switzerland). The fluorescence was monitored at 460 nm ($\lambda_{ex} = 360$ nm) for 90 min at 37 °C. The progress of the reactions was recorded and the initial linear ranges were used to calculate the velocity. IC50 values were calculated in Prism (GraphPad Software, CA, USA) and are means from at least three independent determinations.

Protein labeling for immunoproteasome ($\beta 5i$) MS analysis:

For the immunoproteasome labelling experiments, isolated $\beta 5i$ subunit was purchased from ProSpec-Tany TechnoGene Ltd, as 22 μ M solution in 20 mM Tris-HCl buffer (pH 8.0), with 0.4 M urea and 10 % glycerol. The peptide solution was filtered through a G25 column and the medium was changed to 50 mM Tris (pH 7.4) with 0.5 mM EDTA and 0.01% SDS. Fragments were added from a 100 mM DMSO stock diluted in the labelling solution to 1 mM. The samples were kept at 37 °C for 5 h, then at room temperature for further 12 h. Finally, the samples were purified on a G25 column.

MS analysis of the labelled immunoproteasome ($\beta 5i$):

The molecular weights of the conjugates of IPS $\beta 5i$ were identified using a Triple TOF 5600 + hybrid Quadrupole-TOF LC/MS/MS system (Sciex, Singapore, Woodlands) equipped with a DuoSpray IonSource coupled with a Shimadzu Prominence LC20 UFLC (Shimadzu, Japan) system consisting of binary pump, an autosampler and a thermostated column compartment. Data acquisition and processing were performed using Analyst TF software version 1.7.1 (AB Sciex Instruments, CA, USA). Chromatographic separation was achieved on a Thermo Beta Basic C8 (50 mm \times 2,1 mm, 3 μ m, 150 Å) HPLC column. Sample was eluted in gradient elution mode using solvent A (0.1 % formic acid in water) and solvent B (0.1% formic acid in ACN). The initial condition was 20% B for 1 min, followed by a linear gradient to 90 % B by 4 min, from 5 to 6 min 90 % B was retained; and from 6 to 6.5 min back to initial condition with 20% eluent B and retained from 6.5 to 9.0 min. Flow rate was set to 0.4 ml/min. The column temperature was 40°C and the injection volume was 5 μ l. Nitrogen was used as the nebulizer gas (GS1), heater gas (GS2), and curtain gas with the optimum values set at 30, 30 and 35 (arbitrary units), respectively. Data were acquired in positive electrospray mode in the mass range of m/z300 to 2500, with 1 s accumulation time. The source temperature was 350°C and the spray voltage was set to 5500 V. Declustering potential value was set to 80 V. Peak View Software TM V.2.2 (version 2.2, Sciex, Redwood City, CA, USA) was used for deconvoluting the raw electrospray data to obtain the neutral molecular masses.

Digestion and proteomics MS/MS analysis:[12a]

After the labelling 40–50 μ L of the sample and 10 μ L 0.2% (w/v) RapiGest SF (Waters, Milford, USA) solution buffered with 50 mM ammonium bicarbonate were mixed (pH 7.8) and 3.3 μ L of 45 mM DTT in 100 mM NH_4HCO_3 were added and kept at 37.5°C for 30 min. After cooling the sample to room temperature, 4.16 μ L of 100 mM iodoacetamide in 100 mM NH_4HCO_3 were added and placed in the dark in room temperature for 30 min. The reduced and alkylated protein was then digested by 10 μ L (1 mg/mL) trypsin (the enzyme/protein ratio was 1: 10; Sigma). The sample was incubated at 37°C for overnight. To degrade the surfactant, 7 μ L of formic acid (500 mM) solution was added to the digested protein sample to obtain the final 40 mM concentration (pH \approx 2) and was incubated at 37°C for 45 min. For LC-MS analysis, the acid treated sample was centrifuged for 5 min at 17 000 g. QTRAP 6500 triple quadrupole-linear ion

trap mass spectrometer, equipped with a Turbo V source in electrospray mode (AB Sciex, CA, USA) and a Perkin Elmer Series 200 micro LC system was used for LC-MS/MS analysis. Data acquisition and processing were performed using Analyst software version 1.6.2 (ABSciex Instruments, CA, USA). Chromatographic separation was achieved by using the Vydac 218 TP52 Protein & Peptide C18 column (250 mm × 2.1 mm, 5 μm). The sample was eluted with a gradient of solvent A (0.1% formic acid in water) and solvent B (0.1% formic acid in ACN). The flow rate was set to 0.2 mL/min. The initial conditions for separation were 5 % B for 7 min, followed by a linear gradient to 90 % B by 53 min, from 60 to 63 min 90% B is retained; from 64 to 65 min back to the initial conditions with 5% eluent B retained to 70 min. The injection volume was 10 μL (300 pmol on the column). Information Dependent Acquisition (IDA) LC-MS/MS experiment was used to identify the modified tryptic peptide fragments. Enhanced MS scan (EMS) was applied as survey scan and enhanced product ion (EPI) was the dependent scan. The collision energy in EPI experiments was set to rolling collision energy mode, where the actual value was set on the basis of the mass and charge state of the selected ion. Further IDA criteria: ions greater than: 400.000 m/z, which exceeds 106 counts, exclude former target ions for 30 s after 2 occurrences. In EMS and in EPI mode the scan rate was 1000 Da/s as well. Nitrogen was used as the nebulizer gas (GS1), heater gas (GS2), and curtain gas with the optimum values set at 50, 40 and 40 (arbitrary units). The source temperature was 350°C and the ion spray voltage set at 5000 V. Declustering potential value was set to 150 V. GPMW 4.2 software and ProteinProspector [29] was used to analyse the large number of MS-MS spectra and identify the modified tryptic peptides.

KRASG12C analysis by Ellman's assay:

To measure thiol-reactivity, 2 μM GDP-bound KRASG12C in assay buffer (25 mM NaH₂PO₄, 0.1 mM EDTA, 150 mM NaCl, pH 6.6) was treated with 200 μM of fragments, resulting in 5 % DMSO concentration in the mixture. After 2 h of incubation on room temperature, 16 μL of the sample was pipetted into a black, 384-well assay plate (Corning, Ref No.: 4514) and 4 μL of thiol detection reagent (Invitrogen, ref no.: TC012-1EA) was added. After brief shaking, the plate was incubated in dark, room temperature for 30 min, then fluorescence was measured in duplicates in a microplate reader (BioTek Synergy Mx; λ_{ex}=390 nm and λ_{em}=510 nm). Free thiol ratio (FTR%) labelling ratio (LR%) values were calculated, as follows:

$$\text{FTR}[\%] = 100 \cdot \frac{\text{RFU}_{\text{sample}} - \text{RFU}_{\text{background}}}{\text{RFU}_{\text{DMSO}} - \text{RFU}_{\text{background}}}$$

$$\text{LR}[\%] = 100 \cdot \frac{\text{RFU}_{\text{DMSO}} - \text{RFU}_{\text{sample}}}{\text{RFU}_{\text{DMSO}} - \text{RFU}_{\text{background}}}$$

KRASG12C analysis by NMR:

NMR measurements for testing binding of BTf compounds to GDP-bound KRASG12C protein were carried out on a Bruker Avance III 700 MHz spectrometer equipped with a 5-mm Prodigy TCI H&F C/N D, z-gradient probe head operating at 700.05 MHz for ¹H and 70.94 MHz for ¹⁵N and 658.71 MHz for ¹⁹F nuclei. Spectra were recorded at 298 K. TFA standard solution contained 0.1% trifluoroacetic acid in H₂O. For NMR samples BTf compounds were dissolved in DMSO in 12 mM concentration. To obtain reference spectra free BTf molecules (without protein) were measured in PBS buffer (pH 7.4), 5 mM MgCl₂, 10 % D₂O and 5% BTf-stock solution (in DMSO)

and 0.2 % TFA standard solution (1 μ L in 500 μ L NMR sample) and for the protein (without BTF molecules) were measured in 15 N-labeled KRAS4B G12C(1–169) (catalytic do-main) mutant in 0.2 mM concentration, 5 mM GDP, 10 mM EDTA, 15 mM MgCl₂ in PBS buffer (pH 7.4), 10 % D₂O, 5 % DMSO and 1% DSS standard. NMR samples for binding tests contained 15 N-labeled KRAS4B G12C(1–169) in 0.2 mM concentration, 5 % BTF-stock solution (in DMSO, the final concentration of the compound is 0.6 mM), 2–3 mM GDP, 3–5 mM EDTA, 8–10 mM MgCl₂ in PBS buffer (pH 7.4), 10 % D₂O and 0.2% TFA standard solution (1 μ L in 500 μ L NMR sample).

In binding tests 1D 19 F-NMR (NS = 4), 1D 1 H NMR (NS = 64) and 2D 1 H, 15 N SOFAST HMQC (NS = 64) spectra containing the very same information as 1 H, 15 N-HSQC spectra were performed subsequently immediately after mixing (i. e., 0.3–1 h) and after 1 day's incubation (22–28 h) at room temperature. In case of those BTF molecules which half lives in PBS + 5 % DMSO buffer were shorter than 24 h according to HPLC measurements, the incubation time was a minimum of 10 times longer than the (estimated) half-life if shorter than 1 day. To obtain reference signals for free BTF molecules, 19 F-NMR spectra were performed with the same parameters as in the binding test after a minimum of 3–4 half-life time incubation and for the free protein a 2D 1 H, 15 N-SOFAST HMQC spectrum was used. Sequence specific assignment of HN and NH in the bound KRASG12C spectra were transferred from previous results.[30] All 1 H chemical shifts were referenced to the DMSO peaks (which were calibrated to DSS resonance before in free protein measurements) as DSS were not added to avoid any side reactions with the limited amount of small molecules. 15 N chemical shift values were referenced indirectly using the corresponding gyromagnetic ratios according to IUPAC convention. 19 F chemical shifts were referenced to the TFA signal corresponding to its CF₃ group. All spectra were processed with Bruker TOPSPIN. Binding was confirmed in every case by both 19 F-NMR and 1 H, 15 N-SOFAST HMQC spectra: based on the BTF compound evidenced by comparing 19 F-NMR spectra of free BTF compound and BTF + protein and KRASG12C demonstrated by comparing 1 H, 15 N-SOFAST HMQC spectra of free KRASG12C-GDP and BTF + protein. Based on the assignment of 1 H, 15 N-SOFAST HMQC spectra KRASG12C-GDP, the cysteines modified covalently by BTF molecules were determined as well.

Syntheses

N-(3,5-Bis(trifluoromethyl)phenyl)acrylamide (1):[31]

Triethylamine (1.40 mL, 10 mmol) was added to a solution of 3,5-bis (trifluoromethyl)aniline (1.56 mL, 10 mmol) in CH₂Cl₂(30 mL), and the mixture was allowed to stir under Ar at room temperature (RT)for 10 min. The mixture was cooled with iced water and the acryloyl chloride (0.81 mL, 10 mmol) was added dropwise, and the reaction was left to stir at RT for 2 h. The reaction was concentrated under vacuum. The residue was diluted with H₂O and extracted with EtOAc. The organic layer was washed with 1 M aq. HCl, dried over Na₂SO₄, filtered, and concentrated under vacuum. The product was washed with Et₂O and then vacuum dried to afford 1 as a white powder (2.06 g, 70%). 1 H NMR (500 MHz, [D₆]DMSO): δ =10.76 (s, 1H, NH), 8.32 (s, 2H, ArH), 7.76 (s, 1H, ArH), 6.37 (qd, J=17.0, 5.9 Hz, 2H, = CH ·), 5.86 ppm (dd, J = 9.7, 2.1 Hz, 1H,= CH-). 19 F NMR (650 MHz, D₂O): δ = - 62.7 ppm.

3,5-Bis(trifluoromethyl)phenyl acrylate (2):

3,5-Bis(trifluoromethyl)phenol (0.15 mL, 1 mmol) and N,N-diisopropylethylamine (0.17 mL, 1 mmol) were dissolved in 10 mL CH₂Cl₂, and the solution was stirred at RT for 10 min. The reaction mixture was cooled with iced water, and then acryloyl chloride (0.08 mL, 1 mmol) was added dropwise. Then the reaction was allowed to stir at RT overnight. The solvent was removed under vacuum and the residue was dissolved in ethyl acetate. The solution was washed with saturated sodium bicarbonate and water. The organic phase was dried over Na₂SO₄, filtered, and concentrated under vacuum. The product was purified by flash column chromatography using a mixture of hexane and ethyl acetate as eluent. The compound 2 was obtained as a colourless oil (39 mg, 14%). ¹H NMR (300 MHz, CDCl₃): δ = 7.82 (s, 1H, ArH), 7.70 (s, 2H, ArH), 6.72 (d, J = 17.2 Hz, 1H, =CH-), 6.39 (dd, J = 17.2, 10.5 Hz, 1H, =CH₂), 6.16 ppm (d, J = 10.4 Hz, 1H, =CH₂). ¹³C NMR (75 MHz, CDCl₃): δ = 163.75, 151.33, 134.47, 133.21 (q, J = 34.1 Hz, 2 C), 127.12, 123.01 (d, J = 272.9 Hz, 2 C), 122.71 (2C), 120.49–119.43 ppm (m). ¹⁹F NMR (650 MHz, D₂O): δ = -64.6 ppm. Anal. calcd. for C₁₁H₆F₆O₂: C, 46.47; H, 2.11. found: C, 46.38; H, 2.15.

3,5-Bis(trifluoromethyl)phenyl propionate (3):

3,5-Bis(trifluoromethyl)phenol (0.15 mL, 1 mmol), dicyclohexylcarbodiimide (0.21 g, 1 mmol), N,N-dimethylaminopyridine (1.2 mg, 0.01 mmol) and propiolic acid (68 μL, 1.1 mmol) were dissolved in CH₂Cl₂ (5 mL) at 0°C, and stirred for 5 h, the colourless solution turning to a yellow suspension. The reaction mixture was quenched with 20 mL of water and separated. The aqueous phase was extracted with dichloromethane (2 × 20 mL). The organic phase was dried over MgSO₄, filtered, and concentrated under vacuum. The product was purified by flash column chromatography using a mixture of hexane and ethyl acetate as eluent. Compound 3 was obtained as a white solid (40 mg, 14%). ¹H NMR (500 MHz, [D₆]DMSO): δ = 8.14 (s, 2H, ArH), 8.05 (s, 1H, ArH), 4.92 ppm (s, 1H, ≡CH). ¹³C NMR (125 MHz, [D₆]DMSO): δ = 150.7, 150.5, 132.1 (q, J = 33.7 Hz, 2 C), 124.2 (d, J = 3.8 Hz, 2 C), 123.1 (q, J = 271.3 Hz, 2 C), 120.8–121.0 (m), 82.9, 74.2 ppm. ¹⁹F NMR (650 MHz, D₂O): δ = -64.7 ppm. Anal. calcd. for C₁₁H₄F₆O₂: C, 46.81; H, 1.42. found: C, 46.67; H, 1.49.

3-(3,5-Bis(trifluoromethyl)phenyl)-2-cyanoacrylamide (4):

[31] 3,5-Bis(trifluoromethyl)benzaldehyde (0.33 mL, 2 mmol) and 2-cyanoacrylamide (252 mg, 3 mmol) were dissolved in methanol (15 mL). To this solution catalytic NaOH (1 mg, 1%) was added, and the reaction was stirred at 45°C for 4 h. The reaction was concentrated under vacuum, followed by adding 25 mL water and 25 mL ethyl acetate to the residue. After separation, the organic layer was washed with brine, dried over Na₂SO₄, filtered, and concentrated under vacuum. The product was obtained as white powder (228 mg, 37%) by column chromatography with a mixture of hexane and ethyl acetate as eluent. ¹H NMR (500 MHz, [D₆]DMSO): δ = 8.54 (s, 2H, ArH), 8.37 (s, 1H, ArH), 8.31 (s, 1H, =CH-), 7.97 (s, 1H, NH₂), 7.89 ppm (s, 1H, NH₂). ¹⁹F NMR (650 MHz, D₂O): δ = -62.7 ppm.

1-(3,5-Bis(trifluoromethyl)phenyl)-1H-pyrrole-2,5-dione (5): [32]

To a solution of maleic anhydride (214 mg, 2.18 mmol) in dichloromethane (20 mL) 3,5-bis(trifluoromethyl)aniline (0.34 mL, 2.2 mmol) was added dropwise at 40 °C, and the mixture was allowed to stir for 2 h. The intermediate was obtained as white crystals (705 mg, 98%) and collected by filtration. The intermediate was dissolved in toluene (30 mL), then catalytical

amount of H₂SO₄ was added (1–2 drops). The reaction flask was equipped with a Dean–Stark apparatus and the mixture was refluxed at 130 °C for 3 h. The solvent was removed under vacuum and the residue was purified by flash column chromatography with a mixture of hexane and ethyl acetate as eluent. The product was obtained as brown solid (272 mg, 40 %). ¹H NMR (500 MHz, [D₆]DMSO): δ = 8.15 (s, 1H, ArH), 8.12 (s, 2H, ArH), 7.27 ppm (s, 2H, =CH–). ¹⁹F NMR (650 MHz, D₂O): δ = 62.7 ppm.

1-(3,5-Bis(trifluoromethyl)benzyl)-1H-pyrrole-2,5-dione (6):

The same procedure as for 5 except using 3,5-bis(trifluoromethyl)benzylamine (535 mg, 2.18 mmol). The product was obtained as brown solid (317 mg, 45 %). ¹H NMR (500 MHz, [D₆]DMSO): δ = 8.27 (s, 2H, ArH), 8.21 (s, 2H, –CH =), 8.11 (s, 1H, ArH), 4.25 ppm (d, J = 5.2 Hz, 2H, CH₂). ¹³C NMR (125 MHz, [D₆]DMSO): δ = 172.5 (2C), 137.7 (2C), 130.8 (2C), 130.7 (q, J = 32.5 Hz), 130.6 (2C), 124.7, 122.5–122.7 (m, 2 C), 41.8 ppm. ¹⁹F NMR (650 MHz, D₂O): δ = 62.5 ppm. HRMS (ESI): [M + H]⁺ calcd. for C₁₃H₇F₆N₂O₂ +, 324.0459; found: 324.0447.

3-(3,5-Bis(trifluoromethyl)phenyl)acrylamide (7):

In a sealed tube 3,4-bis(trifluoromethyl)bromobenzene (0.35 mL, 2 mmol), acrylamide (171 mg, 2.4 mmol), Pd(OAc)₂ (11 mg, 0.05 mmol), diisopropylethyl-amine (0.42 mL, 2.4 mmol) and tri(o-tolyl)phosphine (30 mg, 0.1 mmol) was added to dimethylformamide (5 mL) under Ar and heated at 130 °C for 1.5 h. The crude mixture was filtered from activated charcoal and water/MeOH 1: 1 was added. The forming yellow crystals were filtered (140 mg, 49 %). ¹H NMR (500 MHz, CDCl₃): δ = 7.92 (s, 2H, ArH), 7.86 (s, 1H, ArH), 7.70 (d, J = 15.7 Hz, 1H, =CH–), 6.60 (d, J = 15.7 Hz, 1H, =CH–), 5.71 ppm (s, 2H, NH₂). ¹³C NMR (125 MHz, CDCl₃): δ = 166.3, 138.3, 136.3 (2C), 131.3 (q, J = 33.0 Hz), 128.4, 128.3, 127.1 (2C), 124.7, 122.5–122.8 ppm (m). ¹⁹F NMR (650 MHz, D₂O): δ = 62.6 ppm. HRMS (ESI): [M + H]⁺ calcd. for C₁₁H₇F₆N₂O : 284.0510; found: 284.0509.

Ethyl 3-(3,5-bis(trifluoromethyl)phenyl)acrylate (8):[33]

In a sealed tube 0.35 mL 3,4-bis(trifluoromethyl)bromobenzene (2 mmol), ethylacrylate (0.26 mL, 2.4 mmol), Pd(OAc)₂ (11 mg, 0.05 mmol), diisopropylethylamine (0.42 mL, 2.4 mmol) and tri(o-tolyl)phosphine (30 mg, 0.1 mmol) was added to dimethylformamide (5 mL) under Ar and heated at 100 °C for 4 h. The crude mixture was filtered from activated charcoal and water/MeOH 1: 1 was added. The forming yellow crystals were filtered (300 mg, 48 %). ¹H NMR (500 MHz, [D₆] DMSO): δ = 8.46 (s, 1H, ArH), 8.08 (s, 2H, ArH), 7.81 (d, J = 16.1 Hz, 1H, =CH–), 7.02 (d, J = 16.1 Hz, 1H, =CH–), 4.20 (q, J = 7.1 Hz, 1H, CH₂), 1.26 ppm (t, J = 7.1 Hz, 2H, CH₃). ¹⁹F NMR (650 MHz, D₂O): δ = 64.5 ppm.

3-(3,5-Bis(trifluoromethyl)phenyl)acrylonitrile (9):

In a sealed tube 3,4-bis(trifluoromethyl)bromobenzene (0.69 mL, 4 mmol), acrylonitrile (0.32 mL, 4.8 mmol), Pd(OAc)₂ (9 mg, 0.04 mmol), diisopropylethyl-amine (0.84 mL, 4.8 mmol) and biphenyl-diisopropylphosphine (24 mg, 0.08 mmol) was added to dimethylacetamide (2 mL) under Ar and heated at 130 °C for 4 h. Then 10 mL water and 20 mL methyl-tert-butylether was added to the reaction mixture and the phases were separated. The organic phase was dried over MgSO₄, filtered, and evaporated to silica. The residue was purified with flash column chromatography with hexane and ethyl acetate eluent mixture to give the product as a white

solid (120 mg, 11%). ¹H NMR (500 MHz, CDCl₃): δ = 7.92 (s, 1H, ArH), 7.88 (s, 2H, ArH), 7.47 (d, J = 16.7 Hz, 1H, = CH-), 6.08 ppm (d, J = 16.7 Hz, 1H, = CH-). ¹³C NMR (125 MHz, CDCl₃): δ = 146.9, 135.4, 133.9 (d, J = 33.8 Hz), 127.3 (q, J = 3.9 Hz), 124.4–124.2 (m), 122.7 (d, J = 272.9 Hz), 116.6, 101.01 ppm. ¹⁹F NMR (650 MHz, D₂O): δ = - 62.8 ppm. HRMS calcd. for C₁₁H₆F₆N: 266.0404; found: 266.0396.

Methyl 3-(3,5-bis(trifluoromethyl)phenyl)propionate (10):[34]

In a sealed tube 3,5-bis(trifluoromethyl)phenylboronic acid (218 mg, 1 mmol), methyl propionate (0.13 mL, 1.5 mmol), copper(I) iodide (29 mg, 0.15 mmol), silver(I) oxide (462 mg, 2 mmol) and caesium carbonate (652 mg, 2 mmol) was dissolved in dichloroethane (5 mL). The reaction mixture was stirred under Ar at 80°C overnight. 10 mL water was added to the mixture then the separated organic layer was washed with brine, dried over Na₂SO₄, filtered, and concentrated under vacuum. The crude product was purified by flash column chromatography with mixture of hexane and ethyl acetate as eluent. The product was obtained as a light brown oil (115 mg, 39%). ¹H NMR (CDCl₃): δ = 8.06 (2H, s, ArH), 7.94 (s, 1H, ArH), 3.88 ppm (3H, CH₃). ¹⁹F NMR (650 MHz, D₂O): δ = - 64.9 ppm.

3,5-Bis(trifluoromethyl)phenyl vinylsulfone (11):[35]

3,5-Bis(trifluoromethyl)thiophenol (505 μL, 3 mmol) and potassium-carbonate (830 mg, 6 mmol) was dissolved in N,N-dimethylformamide (25 mL), then 2-chloroethanol (270 μL, 4 mmol) was added and the mixture was stirred at RT. After 4 hours, the solvent was evaporated and the residue was dissolved in 50 mL ethyl acetate, then washed with 50 mL brine. The organic layer was dried and concentrated. The crude product was dissolved in 30 mL dichloromethane and meta-chloroperoxybenzoic acid (1.29 g, 7.5 mmol) was added slowly. The mixture was stirred for 3 h, then it was washed with 1 M aqueous solution of sodium hydroxide. After the extraction the organic phase was dried and concentrated, then the product was dissolved in 20 mL dry dichloromethane. To this solution methanesulfonyl-chloride (230 μL, 3 mmol) was added at 0°C, then triethylamine (625 μL, 4.5 mmol) was dropped slowly into the mixture. After the addition of the base, the reaction was heated up to RT and stirred for 3 h. Finally, the solvent was removed and the crude product was purified by column chromatography to give the 11 vinylsulfone product (128 mg, 14%) ¹H NMR (500 MHz, [D₆]DMSO): δ = 8.34 (s, 2H), 8.13 (s, 1H), 6.74–6.61 (m, 2H), 6.24 ppm (d, J = 8.7 Hz, 1H). ¹⁹F NMR (650 MHz, D₂O): δ = - 62.8 ppm.

3,5-Bis(trifluoromethyl)benzyl vinylsulfone (12):

3,5-Bis(trifluoromethyl)benzyl chloride (1313 mg, 5 mmol) in N,N-dimethylformamide (10 mL) was added dropwise to the solution of 2-mercaptoethanol (350 μL, 5 mmol) and potassium carbonate (1037 mg, 7.5 mmol) in N,N-dimethylformamide (20 mL), then the mixture was stirred at RT. After 3 h, the solvent was evaporated and the residue was dissolved in 50 mL ethyl acetate, then washed with 50 mL brine. The organic layer was dried and concentrated. The crude product was dissolved in 50 mL dichloromethane and meta-chloroperoxybenzoic acid (2.16 g, 12.5 mmol) was added slowly. The mixture was stirred for 3 h, and then it was washed with 1 M aqueous solution of sodium hydroxide. After the extraction the organic phase was dried and concentrated, then the product was dissolved in 20 mL dry CH₂Cl₂. To this solution methanesulfonyl-chloride (464 μL, 6 mmol) was added at 0°C, and triethylamine (1043 μL, 7.5 mmol) was dropped slowly into the mixture. After the addition of the base, the reaction mixture

was heated up to RT and stirred for 2 h. Finally, the solvent was removed and the product was purified by column chromatography to obtain 12 as a white powder (328 mg, 21 %). ¹H NMR (500 MHz, [D₆]DMSO): δ = 8.14 (s, 1H), 8.09 (s, 2H), 7.00 (dd, J = 16.6, 10.0 Hz, 1H), 6.26 (d, J = 9.9 Hz, 1H), 6.08 (d, J = 16.6 Hz, 3H), 4.84 ppm (s, 6H). ¹³C NMR (125 MHz, CDCl₃): δ = 136.4, 132.8, 132.2 (2C), 131.8, 130.7 (q, J = 32.5 Hz, 2 C), 123.6 (q, J = 271.3 Hz, 2 C), 122.8–122.6 (m), 57.9 ppm. ¹⁹F NMR (650 MHz, D₂O): δ = - 62.6 ppm. HRMS (DUIS): [M- H]⁻ calcd. for C₁₁H₇F₆O₂S⁻: 317.0076; found: 317.0046.

***N*-(3,5-Bis(trifluoromethyl)benzyl)ethanesulfonamide (13):**

To a stirred solution of 3,5-bis(trifluoromethyl)benzyl amine (1215 mg, 5 mmol) and trimethylamine (2087 μL, 15 mmol) in CH₂Cl₂ (40 mL) at 0°C, 2-chloroethanesulfonylchloride (1045 μL, 10 mmol) was added drop-wise. The resulting mixture was then stirred at 0°C until the amine was consumed as determined by TLC. The reaction was quenched with water (300 mL) and the mixture was extracted with CH₂Cl₂ (3×25 mL). The combined organic extracts were washed with brine (10 mL), dried with anhydrous Na₂SO₄. The solvent was removed under vacuum and the residue was purified by column chromatography with a mixture of hexane and ethyl acetate as the eluent, to give the product as a white powder (882 mg, 53 %). ¹H NMR (500 MHz, [D₆]DMSO): δ = 8.04 (t, J = 6.3 Hz, 1H), 8.03 (s, 2H), 8.00 (s, 1H), 6.74 (dd, J = 16.5, 10.0 Hz, 1H), 6.06 (d, J = 16.5 Hz, 1H), 5.98 (d, J = 10.0 Hz, 1H), 4.28 ppm (d, J = 6.3 Hz, 2H). ¹³C NMR (125 MHz, [D₆]DMSO): δ = 147.3, 142.0, 135.4 (q, J = 32.5 Hz, 2 C), 133.6 (2C), 131.2, 128.5 (q, J = 271.3 Hz, 2 C), 126.3–126.0 (m), 49.9 ppm. ¹⁹F NMR (650 MHz, D₂O): δ = - 62.6 ppm. HRMS (DUIS): [M- H]⁻ calcd. for C₁₁H₈F₆N₂O₂S⁻: 332.0185; found: 332.0157.

1-(Isothiocyanatomethyl)-3,5-bis(trifluoromethyl)benzene (15):

In a round bottom flask 1,1'-thiocarbonylbis(pyridin-2(1H)-one) (3 mmol, 0.7 g) was dissolved in CH₂Cl₂ (100 mL). 3,5-Bistrifluoromethylbenzylamine (0.24 g, 1 mmol) was dissolved in dichloromethane (50 mL) and added dropwise. The reaction mixture was stirred at RT for 50 min. Then the reaction mixture was washed with brine (2 × 20 mL) and 1 M HCl (20 mL), and the organic phase was dried over MgSO₄. The solvent was evaporated, and the crude product was purified with flash column chromatography using hexane and ethyl acetate as the eluent (9: 1) resulting in the product as a colourless oil (171 mg, 60 %). ¹H NMR (500 MHz, CDCl₃): δ = 7.88 (s, 1H, ArH), 7.79 (s, 2H, ArH), 4.89 ppm (s, 2H, CH₂). ¹³C NMR (125 MHz, CDCl₃) 185.4 (d, J = 338.6 Hz), 140.0, 132.2 (d, J = 33.5 Hz), 127.7–127.5 (m), 124.1, 122.0–121.7 (m), 47.6 ppm. ¹⁹F NMR (650 MHz, D₂O): δ = - 64.4 ppm. HRMS (DUIS): [M- H]⁻ calcd. for C₁₀H₄F₆NS⁻: 283.9968; found: 283.9967.

***tert*-Butyl 2-(3,5-bis(trifluoromethyl)benzylidene)hydrazine carboxylate (19):**

3,5-Bis(trifluoromethyl)benzaldehyde (0.16 mL, 1 mmol) and *tert*-butyl hydrazinecarboxylate (145 mg, 1.1 mmol) were dissolved in 1 : 1 mixture of tetrahydrofuran and dichloromethane (30 mL). Then catalytic amount of H₂SO₄ (1–2 drops) was added and the reaction was stirred at RT for 2 h. The solvent was removed under vacuum, then crude product was filtered through a silica pad using dichloromethane-methanol solvent mixture. Then 25 mL water and 25 mL ethyl acetate was added to the residue. After the separation, the organic layer was washed with brine, dried over Na₂SO₄, filtered, and concentrated under vacuum. The product was obtained by flash column chromatography with a mixture of hexane and ethyl acetate as the eluent. The product

was obtained as a yellow powder (281 mg, 78%). ¹H NMR (500 MHz, [D₆]DMSO): δ = 11.29 (s, 1H, NH), 8.25 (s, 2H, ArH), 8.15 (s, 1H, ArH), 8.05 (s, 1H, =CH-), 1.46 ppm (s, 9H, CH₃). ¹³C NMR (125 MHz, [D₆]DMSO): δ = 152.7, 138.0 (2C), 131.2 (q, J = 33.1 Hz, 2 C), 126.9–127.1 (m, 3 C), 124.7, 122.6, 80.4, 29.4 ppm (3 C). ¹⁹F NMR (650 MHz, D₂O): δ = 62.7 ppm. HRMS (ESI): [M + H]⁺ calcd. for C₁₄H₁₄F₆N₂O₂ + : 357.1037; found: 357.1039.

***N*-(3,5-Bis(trifluoromethyl)benzyl)cyanamide (20):**

To a cooled solution (0 °C) of 3,5-bis(trifluoromethyl)benzyl amine (486 mg, 2 mmol) in dry diethyl ether (20 mL) cyanogen bromide as 3 M solution in CH₂Cl₂ (100 μL, 2 mmol) was added dropwise. The reaction was warmed to RT and stirred for 16 h. The mixture was filtered to remove the residual salt and the filtrate was concentrated. The residue was diluted in 25 mL ethyl acetate, washed with water (30 mL) and brine (30 mL). Organic extracts was dried over Na₂SO₄, filtered, and concentrated under vacuum. The product was obtained by flash column chromatography with a mixture of hexane and ethyl acetate as the eluent. Compound 20 was obtained as a white solid (453 mg, 34%). ¹H NMR (500 MHz, [D₆] DMSO): δ = 8.05 (s, 1H), 7.41 (s, 1H), 4.34 ppm (d, J = 4.0 Hz, 1H). ¹³C NMR (125 MHz, CDCl₃): δ = 142.0, 130.9 (q, J = 32.8 Hz, 2 C), 129.0 (2C), 123.7 (q, J = 268.3 Hz, 2 C), 122.7–121.9 (m), 117.2, 47.6 ppm. ¹⁹F NMR (650 MHz, D₂O): δ = - 62.5 ppm. HRMS (DUIS): [M - H]⁻ calcd. for C₁₀H₅F₆N₂: 267.0362; found: 267.0325.

***N*-(3,5-Bis(trifluoromethyl)phenyl)-2-chloroacetamide (21):[36]**

The same procedure as for 1 except using chloroacetyl chloride (0.80 mL, 10 mmol). Pure 21 was obtained as a white powder (2.31 g, 75 %). ¹H NMR (500 MHz, [D₆]DMSO): δ = 10.90 (s, 1H, NH), 8.24 (s, 2H, ArH), 7.80 (s, 1H, ArH), 4.32 ppm (s, 2H, CH₂Cl). ¹⁹F NMR (650 MHz, D₂O): δ = - 62.7 ppm.

***N*-(3,5-Bis(trifluoromethyl)phenyl)-2-chloropropanamide (22):[31]**

The same procedure as for 1 except using 2-chloropropanoyl chloride (0.97 mL, 10 mmol) and the reaction mixture was allowed to stir at RT overnight. Crude product was purified by flash column chromatography with a mixture of hexane and ethyl acetate as an eluent to give the pure product as a white powder (1.35 g, 42%). ¹H NMR (500 MHz, CDCl₃): δ = 10.21 (s, 1H, NH), 8.34 (s, 2H, ArH), 7.68 (s, 1H, ArH), 5.38 (q, J = 7.0 Hz, 1H, CHCl), 1.99 ppm (d, J = 7.1 Hz, 3H, CH₃). ¹⁹F NMR (650 MHz, D₂O): δ = - 62.7 ppm.

***N*-(3,5-Bis(trifluoromethyl)phenyl)-2-bromopropanamide (23):[31]**

The same procedure as for 1 except using 2-bromopropanoyl chloride (1.01 mL, 10 mmol), and the reaction mixture was allowed to stir at RT for 2 days. Crude product was purified by flash column chromatography with a mixture of hexane and ethyl acetate as an eluent to give the pure product as a brown powder (1.38 g, 38 %). ¹H NMR (500 MHz, [D₆]DMSO): δ = 10.95 (s, 1H, NH), 8.25 (s, 1H, ArH), 7.78 (s, 1H, ArH), 4.67 (q, J = 6.7 Hz, 1H, CHBr), 1.76 ppm (d, J = 6.7 Hz, 1H, CH₃). ¹⁹F NMR (650 MHz, D₂O): δ = - 62.7 ppm.

***1*-(3,5-Bis(trifluoromethyl)phenyl)-2-bromoethanone (24):[37]**

To a stirred solution of 3',5'-bis(trifluoromethyl)acetophenone (0.18 mL, 1 mmol) in THF (10 mL) pyridinium tribromide (0.32 mL, 1 mmol) dissolved in THF (10 mL) was added dropwise. The reaction mixture was stirred for 4 h. Water (20 mL) was added, and the phases were separated.

The aqueous phase was extracted with ethyl acetate (2×20 mL). The organic phase was dried over MgSO₄ and evaporated. Flash column chromatography using hexane/ethyl acetate (95 : 5) as the eluent afforded the product as a yellow oil that solidified overnight (190 mg, 57 %). ¹H NMR (500 MHz, [D₆]DMSO): δ = 8.55 (s, 2H, ArH), 8.44 (s, 1H, ArH), 5.12 ppm (s, 2H, CH₂Br). ¹⁹F NMR (650 MHz, D₂O): δ = -62.7 ppm.

2-(3,5-Bis(trifluoromethyl)phenyl)oxirane (25):[38]

3,5-Bistrifluoromethylphenyl-styrene (0.36 mL, 2 mmol) was dissolved in chloroform (20 mL), and meta-chloroperoxybenzoic acid (1.38 g, 4 mmol) was added at 0°C. The reaction mixture was stirred overnight, followed by washing with saturated NaHCO₃ (10 mL). The organic phase was dried over MgSO₄ and evaporated. The crude product was purified with flash chromatography using hexane/ethyl acetate (93:7) as the eluent, resulting in the product as a colourless oil (364 mg, 71%). ¹H NMR (500 MHz, CDCl₃): δ = 7.82 (s, 1H, ArH), 7.74 (s, 2H, ArH), 3.99 (dd, J = 3.8, 2.6 Hz, 1H, CH₂O), 3.23 (dd, J = 5.3, 4.1 Hz, 1H, CH₂O), 2.79 ppm (dd, J = 5.4, 2.4 Hz, 1H, CH₂O). ¹⁹F NMR (650 MHz, D₂O): δ = -62.6 ppm.

Acknowledgements

The research was funded by H2020 MSCA Fragnet (project 675899), SNN 125496, OTKA PD124598 and 2018-2.1.11-TÉT SI-2018-00005, NVKP_16-1-2016-0020 and NKP-2018-1.2.1-NKP-2018-00005 (National Research, Development and Innovation Office of Hungary), the ELTE Thematic Excellence Programme and BME-Biotechnology FIKP grant (BME FIKP-BIO) supported by the Hungarian Ministry for Innovation and Technology, the Slovenian Research Agency (grants Z1-1859, N1-0068, J3-1745, J1-8145 and P1-0208), and a grant from the Hessian Landes-Offensive zur Entwicklung Wissenschaftlich-ökonomischer Exzellenz (LOEWE TRABITA). K.N. was supported by the ÚNKP-20-4 (ÚNKP-20-4-II-BME-311) New National Excellence Program of the Ministry for Innovation and Technology from the source of the National Research, Development and Innovation Fund. The work of A. Scarpino, K. Németh, G. Koppány and I. Vida is gratefully acknowledged.

Conflict of Interest

The authors declare no conflict of interest.

Keywords: drug design · electrophilic warheads · KRASG12C · MAO · targeted covalent inhibitors

- [1] a) T. A. Baillie, *Angew. Chem. Int. Ed.* **2016**, *55*, 13408–13421; *Angew. Chem.* **2016**, *128*, 13606–13619; b) R. A. Bauer, *Drug Discovery Today* **2015**, *20*, 1061–1073; c) A. Vasudevan, M. A. Argiriadi, A. Baranczak, M. Friedman, J. Gavrilyuk, A. D. Hobson, J. J. Hulce, S. Osman, N. S. Wilson, *Prog. Med. Chem.* **2019**, *58*, 1–62.
- [2] D. A. Shannon, E. Weerapana, *Curr. Opin. Chem. Biol.* **2015**, *24*, 18–26.
- [3] a) A. J. T. Smith, X. Zhang, A. G. Leach, K. N. Houk, *J. Med. Chem.* **2009**, *52*, 225–233; b) C. González-Bello, *ChemMedChem* **2016**, *11*, 22–30.
- [4] A. Tuley, W. Fast, *Biochemistry* **2018**, *57*, 3326–3337.
- [5] M. Gersch, J. Kreuzer, S. A. Sieber, *Nat. Prod. Rep.* **2012**, *29*, 659–682.
- [6] a) T. Zhang, J. M. Hatcher, M. Teng, N. S. Gray, M. Kostic, *Cell Chem. Biol.* **2019**, *26*, 1486–1500; b) M. Gehringer, S. A. Laufer, *J. Med. Chem.* **2019**, *62*, 5673–5724; c) J. S. Martin-Claire, J. McKenzie, D. F. Ian, H. Gilbert, *Bioorg. Med. Chem.* **2019**, *27*, 2066–2074.
- [7] S. G. Kathman, A. V. Statsyuk, *MedChemComm* **2016**, *7*, 576–585.
- [8] a) A. M. Embaby, S. Schoffelen, C. Kofoed, M. Meldal, F. Diness, *Angew. Chem. Int. Ed.* **2018**, *57*, 8022–8026; *Angew. Chem.* **2018**, *130*, 8154–8158; b) P. Martín-Gago, C. A. Olsen, *Angew. Chem. Int. Ed.* **2019**, *58*, 957–966.
- [9] E. Weerapana, C. Wang, G. M. Simon, F. Richter, S. Khare, M. B. D. Dillon, D. A. Bachovchin, K. Mowen, D. Baker, B. F. Cravatt, *Nature* **2010**, *468*, 790–795.
- [10] a) W. Zhang, J. Pei, L. Lai, *J. Chem. Inf. Model.* **2017**, *57*, 1453–1460; b) E. Awoonor-Williams, C. N. Rowley, *J. Chem. Inf. Model.* **2018**, *58*, 1935–1946; c) R. Liu, Z. Yue, C. C. Tsai, J. Shen, *J. Am. Chem. Soc.* **2019**, *141*, 6553–6560; d) Z. Zhao, Q. Liu, S. Bliven, L. Xie, P. E. Bourne, *J. Med. Chem.* **2017**, *60*, 2879–2889.
- [11] a) E. Resnick, A. Bradley, J. Gan, A. Douangamath, T. Krojer, R. Sethi, P. P. Geurink, A. Aimon, G. Amitai, D. Bellini, J. Bennett, M. Fairhead, O. Fedorov, R. Gabizon, J. Gan, J. Guo, A. Plotnikov, N. Reznik, G. F. Ruda, L. Díaz-Sáez, V. M. Straub, T. Szommer, S. Velupillai, D. Zaidman, Y. Zhang, A. R. Coker, C. G. Dowson, H. M. Barr, C. Wang, K. V. M. Huber, P. E. Brennan, H. Ovaa, F. von Delft N London, *J. Am. Chem. Soc.* **2019**, *141*, 8951–8968; b) A. Keeley, L. Petri, P. Ábrányi-Balogh, G. M. Keserü, *Drug Discovery Today* **2020**, *25*, 983–996.
- [12] a) P. Ábrányi-Balogh, L. Petri, T. Imre, P. Szijj, A. Scarpino, M. Hrast, A. Mitrović, U. P. Fonovič, K. Németh, H. Barreteau, D. I. Roper, K. Horváti, G. G. Ferenczy, J. Kos, J. Ilaš, S. Gobec, G. M. Keserü, *Eur. J. Med. Chem.* **2018**, *160*, 94–107; b) E. H. Krenske, R. C. Petter, K. N. Houk, *J. Org. Chem.* **2016**, *81*, 11726–11733; c) V. J. Cee, L. P. Volak, Y. Chen, M. D. Bartberger, C. Tegley, T. Arvedson, J. McCarter, A. S. Tasker, C. Fotsch, *J. Med. Chem.* **2015**, *58*, 9171–9178; d) R. Lonsdale, J. Burgess, N. Colclough, N. L. Davies, E. M. Lenz, A. L. Orton, R. A. Ward, *J. Chem. Inf. Model.* **2017**, *57*, 3124–3137; e) A. A. Adhikari, T. C. M. Seegar, S. B. Ficarro, M. D. McCurry, D. Ramachandran, L. Yao, S. N. Chaudhari, S. Ndousse-Fetter, A. S. Banks, J. A. Marto, S. C. Blacklow, A. S. Devlin, *Nat. Chem. Biol.* **2020**, *16*, 318–326.

- [13] a) A. Liu, X. Wang, X. Ou, M. Huang, C. Chen, S. Liu, L. Huang, X. Liu, C. Zhang, Y. Zheng, Y. Ren, L. He, J. Yao, *J. Agric. Food Chem.* **2008**, *56*, 6562–6566; b) B. Lallemand, F. Chaix, M. Bury, C. Bruyère, J. Ghostin, J.-P. Becker, C. Delporte, M. Gelbcke, V. Mathieu, J. Dubois, M. Prévost, L. Jabin, R. Kiss, *J. Med. Chem.* **2011**, *54*, 6501–6513.
- [14] M. E. Flanagan, J. A. Abramite, D. P. Anderson, A. Aulabaugh, U. P. Dahal, A. M. Gilbert, C. Li, J. Montgomery, S. R. Oppenheimer, T. Ryder, B. P. Schuff, D. P. Uccello, G. S. Walker, Y. Wu, M. F. Brown, J. M. Chen, M. M. Hayward, M. C. Noe, R. S. Obach, L. Philippe, V. Shanmugasundaram, M. J. Shapiro, J. Starr, J. Stroh, Y. Che, *J. Med. Chem.* **2014**, *57*, 10072–10079.
- [15] I. M. Serafimova, M. A. Pufall, S. Krishnan, K. Duda, M. S. Cohen, R. L. Maglathlin, J. M. McFarland, R. M. Miller, M. Frödin, J. Taunton, *Nat. Chem. Biol.* **2012**, *8*, 471–476.
- [16] H. Han, Y. Yang, S. H. Olesen, A. Becker, S. Betzi, E. Schönbrunn, *Biochemistry* **2010**, *49*, 4276–4282.
- [17] L. De Colibus, M. Li, C. Binda, A. Lustig, D. E. Edmondson, A. Mattevi, *Proc. Natl. Acad. Sci. USA* **2005**, *102*, 12684–12689.
- [18] A. Chakrabarti, I. Oehme, O. Witt, G. Oliveira, W. Sippl, C. Romier, R. J. Pierce, M. Jung, *Trends Pharmacol. Sci.* **2015**, *36*, 481–492.
- [19] O. Witt, H. E. Deubzer, T. Milde, I. Oehme, *Cancer Lett.* **2009**, *277*, 8–21.
- [20] M. Muth, N. Jänsch, A. Koprancovic, A. Krämer, N. Wössner, M. Jung, F. Kirschhöfer, G. Brenner-Weiß, F.-J. Meyer-Almes, *Biochim. Biophys. Acta Gen. Subj.* **2019**, *1863*, 577–585.
- [21] T. A. Thibaudeau, D. M. Smith, *Pharmacol. Rev.* **2019**, *71*, 170–197.
- [22] J. M. L. Ostrem, K. M. Shokat, *Nat. Rev. Drug Discovery* **2016**, *15*, 771–785.
- [23] R. J. Simpson, *CSH. Protoc.* **2008**, *pdb.prot4699*.
- [24] K. Rožman, S. Lešnik, B. Brus, M. Hrast, M. Sova, D. Patin, H. Barreteau, J. Konc, D. Janežič, S. Gobec, *Bioorg. Med. Chem. Lett.* **2017**, *27*, 944–949.
- [25] O.-M. Bautista-Aguilera, A. Samadi, M. Chioua, K. Nikolic, S. Filipic, D. Agbaba, E. Soriano, L. de Andrés, M. I. Rodríguez-Franco, S. Alcaro, R. R. Ramsay, F. Ortuso, M. Yañez, J. Marco-Contelles, *J. Med. Chem.* **2014**, *57*, 10455–10463.
- [26] H. von der Eltz, H.-J. Guder, K. Muehlegger, *US4900822* **1990**.
- [27] M. Li, F. Hubálek, P. Newton-Vinson, D. E. Edmondson, *Protein Expression Purif.* **2002**, *24*, 152–162.
- [28] F. Hubálek, J. Pohl, D. E. Edmondson, *J. Biol. Chem.* **2003**, *278*, 28612–28618.
- [29] <http://prospector.ucsf.edu/prospector/mshome.htm> (retrieved on 10.8.2020).
- [30] G. Pálffy, I. Vida, A. Perczel, *Biomol. NMR Assign.* **2020**, *14*, 1–7.
- [31] B. F. Cravatt, WO2017210600/A1, **2017**.
- [32] R. Callahan, O. Ramirez, K. Rosmarion, R. Rothchild, K. C. Bynum, *J. Heterocycl. Chem.* **2005**, *42*, 889–898.
- [33] Y.-H. Zhang, B.-F. Shi, J.-Q. Yu, *J. Am. Chem. Soc.* **2009**, *131*, 5072–5074.
- [34] A. W.-H. Cheung, S. B. Ferguson, L. H. Foley, A. J. Lovey, US6310247/B1, **2001**.
- [35] L. Al-Riyami, M. A. Pineda, J. Rzepecka, J. K. Huggan, A. I. Khalaf, C. J. Suckling, F. J. Scott, D. T. Rodgers, M. M. Harnett, W. Harnett, *J. Med. Chem.* **2013**, *56*, 9982–10002.
- [36] T. R. K. Reddy, C. Li, X. Guo, P. M. Fischer, L. V. Dekker, *Bioorg. Med. Chem.* **2014**, *22*, 5378–5391.
- [37] Z.-W. Chen, D.-N. Ye, M. Ye, Z.-G. Zhou, S.-H. Li, L.-X. Liu, *Tetrahedron Lett.* **2014**, *55*, 1373–1375.
- [38] S. A. Weissman, K. Rossen, P. J. Reider, *Org. Lett.* **2001**, *3*, 2513–2515.